Supporting Information

Chromium nitride /carbon nanocapsules containing carbon nitride hybrid as Pt-free electrocatalyst for oxygen reduction

Lu Zhao, Lei Wang,* Peng Yu, Dongdong Zhao, Chungui Tian, He Feng, Jing Ma and Honggang Fu*

Experimental section:

1. Synthesis

1.1 Synthesis of CrN/GC hybrid

In a typical synthesis, 10 g of polyacrylic weak-acid anion-exchanged resin (PWAR) was exchanged with 100 mL of 0.1 M $K_3[Fe(CN)_6]/K_2Cr_2O_7$ (1:1) mixture solution and stirred for 20 h, then the PWAR-$Cr_2O_7^{2-}$-$[Fe(CN)_6]^{3-}$ precursor was obtained. Subsequently, 2.5 g of the obtained precursor was added into 50 mL isobutanol and stirred for 0.5 h. Then the above suspension was transferred into a Teflon-lined stainless steel autoclave and kept at 180 ^oC for 4 h. After filtering, washing and drying, and then dried at 60 ^oC for 2 h in air. Afterwards, the product was nitrided under NH_3 atmosphere with a heating rate of 5 K min^{-1} at 900^oC for 6h. Finally, the CrN/GC-2-900 hybrid was obtained after treating with hydrochloric acid solution to remove the Fe species completely. In order to study the effect of heated temperature and CrN content on the ORR performance, the other compared samples were also synthesized (the detailed experimental parameters were displayed in Table S1). The resulting hybrids were denoted as CrN/GC-c-T, in which c stands for different concentrations of $Cr_2O_7^{2-}$ ions in the initial ion-exchanged solution, T stands for the nitrided temperature.

1.2 Synthesis of GC

For comparison the effect of CrN on the ORR performance in the hybrid, the graphitic carbon (GC) without CrN was synthesized as the same condition of CrN/GC-2-900 only in the absence of $K_2Cr_2O_7$ to obtain GC.

Table S1. The experiments parameters for all the compared samples.

Samples name	Pyrolyzation temperature (°C)	Ion-exchanged concentration of $Cr_2O_7^{2-}$ (M)	Ion-exchangd concentration of $[Fe(CN)_6]^{3-}$ (M)	CrN content in the samples calculated from TG(%)
CrN/GC-1-900	900	0.03	0.05	9.38
CrN/GC-2-900	900	0.05	0.05	50.7
CrN/GC-3-900	900	0.06	0.05	67.3
CrN/GC-2-800	800	0.05	0.05	59.6
CrN/GC-2-1000	1000	0.05	0.05	57.2
GC	900	0	0.05	—

2. Characterizations

X-ray diffraction (XRD) analyses were performed on a Bruker D8 Advance diffractometer equipped with Cu Kα (λ = 1.5406 Å) radiation and a LynxEye Detector. Raman spectra were taken out with a Jobin Yvon HR 800 micro-Raman spectrometer at 457.9 nm. TG analysis was tested by using a SDT Q600 instrument with a constant flow of air (flow rate: 100 mL min^{-1}), and the temperature was raised from room temperature to 973 K at a heat rate of 10 K min^{-1}). X-ray photoemission spectroscopy (XPS) studies were carried out on a Kratos-AXIS UL TRA DLD with Al Kα radiation source. Transmission electron microscopy (TEM) characterization was tested on a JEM-2100 electron microscope (JEOL) with an acceleration voltage of 200 kV. The nitrogen adsorption-desorption isotherms were performed by using a Micromeritics TriStar II.

3. Electrochemical mesurements

3.1 Preparation of the working electrode

Typically, a predetermined amount of the corresponding electrocatalyst was dispersed in 1.5 mL ethanol and 0.5 mL of 0.5 wt.% Nafion suspension (DuPont, USA) under sonication, a well-dispersed electrocatalyst “ink” was obtained. Then, 30 μL of the electrocatalyst as-prepared ink was dropped onto the surface of the glassy

carbon disk of the rotating ring-disk electrode (RRDE) or ring-disk electrode (RDE) and dried before electrochemical measurement. The RRDE voltammograms were tested by a RRDE with a Pt ring (inner/outer-ring diameter: 6.25/7.92 mm) and a glassy carbon disk (diameter: 5.61 mm). The LSV curves were recorded by a RDE with a glassy carbon disk (diameter: 5 mm).

3.2 Electrochemical tests

The catalytic activity of the electrocatalysts for the ORR was carried out with a three-electrode system by using a Pine Instrument biopotentiostat. A RRDE with a Pt ring and a glassy carbon disk was used as the working electrode. Platinum foil (1.0 cm^2) and a home-made reversible hydrogen electrode (RHE) were used as the counter electrode and the reference electrode, respectively. The ORR activities of the electrocatalysts were tested in O_2-saturated 0.1 M KOH aqueous solution in the potential range of 0.1–1.1 V (vs RHE) with a scan rate of 5 mV s^{-1}. The ring potential was held at 1.2 V versus RHE. The specific kinetic current densities (J_k) associated with the intrinsic activity of the catalysts can be obtained by Koutecky-Levich equation (1):

$$\frac{1}{j} = \frac{1}{j_k} + \frac{1}{j_d} = \frac{1}{j_k} + \frac{1}{B\omega^{1/2}} \quad (1)$$

where j_k is the kinetic current density, j_d is the diffusion-limited current density, ω is the angular frequency of rotation. The B parameter is defined as eqution (2):

$$B = 0.62\ n\ F\ C_0\ D_0^{3/2} \upsilon^{-1/6} \quad (2)$$

where n is the overall number of electrons, F is the Faraday constant (96485 C mol^{-1}), C_o is the concentration of molecular oxygen in the electrolyte (1.2×10^{-6} mol cm^{-3}), D_o is the diffusion coefficient of the molecular O_2 in 0.1 M KOH solution (1.9×10^{-5} cm^2 s^{-1}), and υ is the viscosity of the electrolyte (0.01 cm^2 s^{-1}).[S1] The electron transfer number (n) were determined by the followed equation (3):

$$n = 4 \times \frac{I_d}{I_d + I_r/N} \quad (3)$$

where Ir is ring current, I_d is disk current, and N is current collection efficiency of the Pt ring; N was determined to be 0.37 from the reduction of $K_4Fe[CN]_6$.

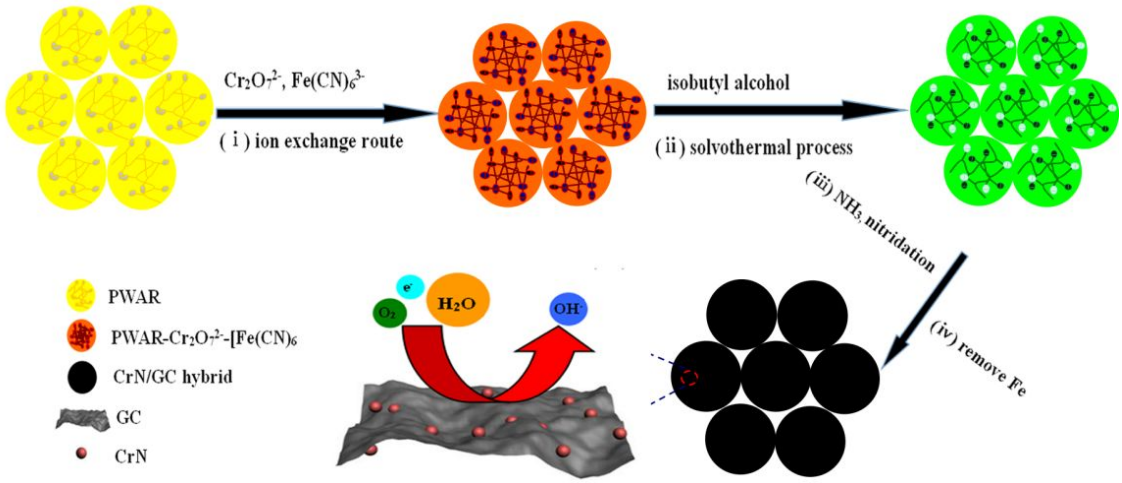

Scheme S1. The synthetic processes of the CrN/GC hybrid.

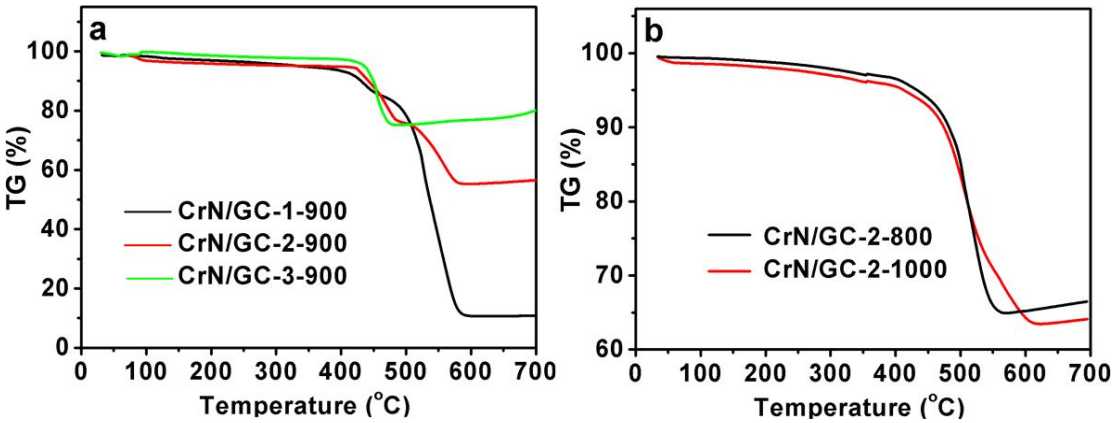

Fig. S1 TG curves of the synthetic CrN/GC hybrids tested in air.

Table S2. TG analyses results derived from Fig. S1.

Samples	Final residual mass after TG tests (Cr_2O_3%)	CrN content calculated based on Cr_2O_3 (%)
CrN/GC-1-900	10.8	9.38
CrN/GC-2-900	56.7	50.7
CrN/GC-3-900	78.5	67.3
CrN/GC-2-800	66.7	59.6
CrN/GC-2-1000	64.1	57.2

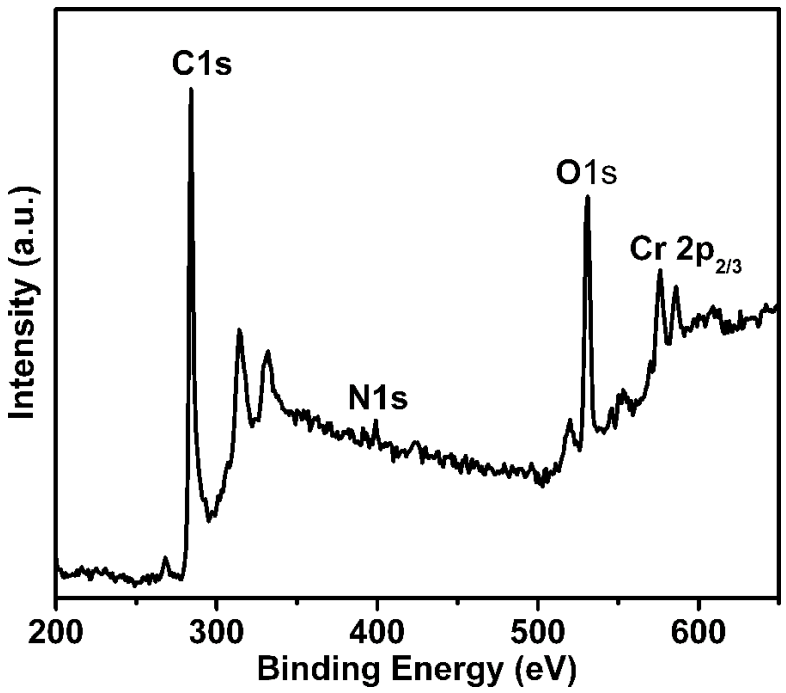

Fig. S2 Wide XPS of the synthetic CrN/GC-2-900 hybrid.

Table S3. Chemical compositions of the synthetic omposites.

Samples name	Weigh (%)					Formula of Carbon nitrides
	Cr (%)[a]	Fe (%)[a]	N (%)[b]	C (%)[b]	CrN (%)	
CrN/GC-1-900	8.12	—	2.67	84.17	10.30	$CN_{0.005}$
CrN/GC-2-900	42.26	—	12.13	40.28	53.64	$CN_{0.016}$
CrN/GC-3-900	52.58	—	15.72	23.84	66.74	$CN_{0.056}$
CrN/GC-2-800	49.05	—	14.86	35.21	62.26	$CN_{0.04}$
CrN/GC-2-1000	46.89	—	13.25	35.63	59.51	$CN_{0.015}$
GC	—	—	1.51	94.76	—	$CN_{0.014}$

Note: [a]Determined by ICP-AES, [b] Determined by elemental analyses.

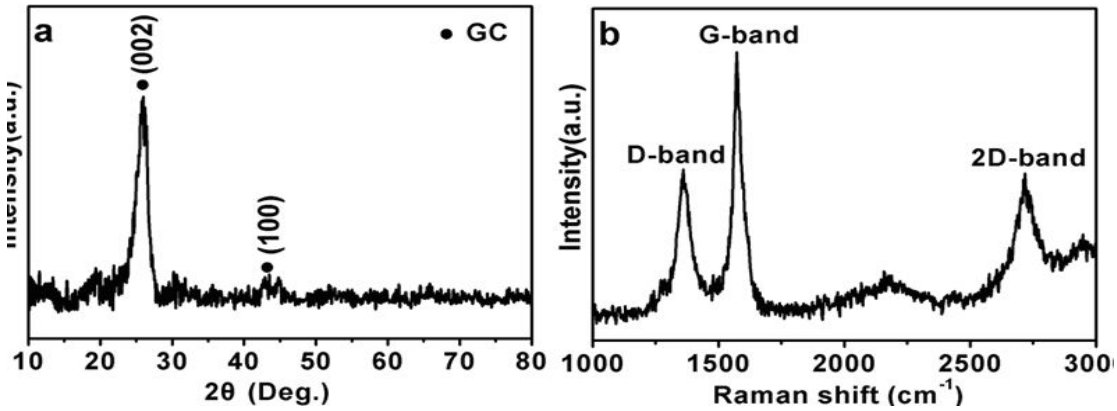

Fig. S3 (a) XRD pattern and (b) Raman spectrum of GC.

For comparing the effect of CrN on the ORR performance, the GC sample derived from the same process as that of CrN/GC-2-900 only without $Cr_2O_7^{2-}$ was prepared. **Fig. S3a** shows the XRD pattern of the synthetic GC, the two characteristic peaks are attributed to the (002) and (100) planes of graphitic carbon. The Raman spectrum in **Fig. S3b** exhibits the typical peak of graphitic carbon, namely the D-band (1355 cm^{-1}), G-band (1571 cm^{-1}) and the intense 2D-band (2720 cm^{-1}), suggesting the high crystallinity of GC.

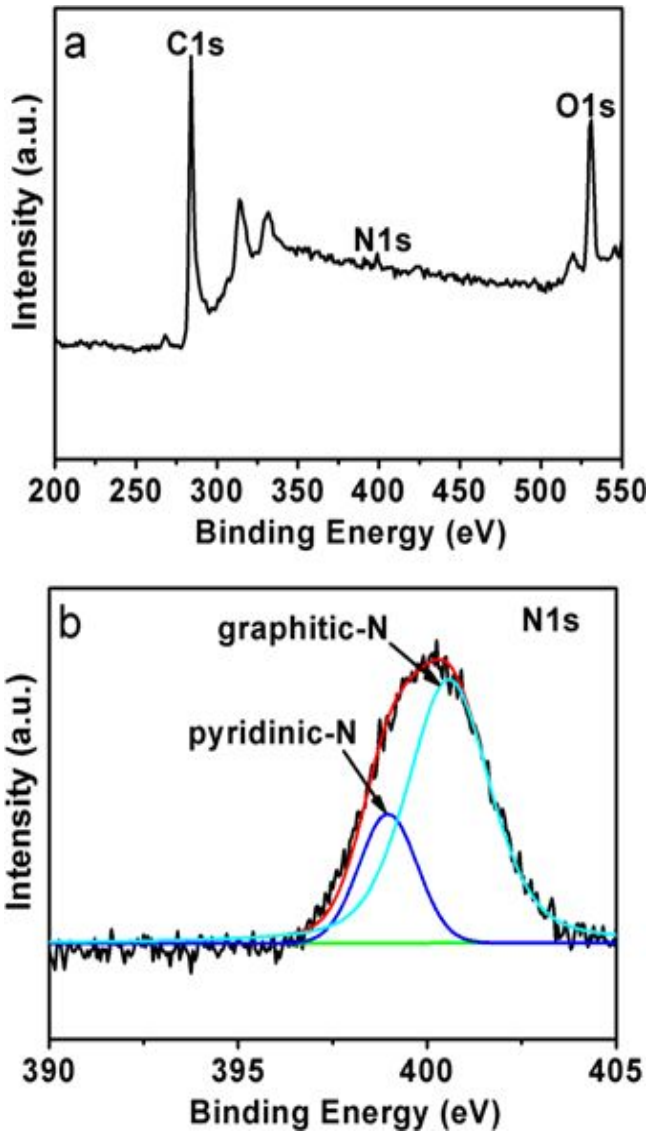

Fig. S4 (a) Wide XPS and (b) high-resolution N1s XPS spectra of GC.

Wide XPS spectrum in **Fig. S4** shows C 1s and N 1s are found with their corresponding binding energies. The N 1s spectra can be deconvoluted into two peaks at 398.5 and 400.6 eV, which are consistent with pyridinic-N and graphitic-N (Fig. S5b), respectively,[S2, S3] implying that nitrogen was indeed doped into the carbon molecular skeletons of GC.

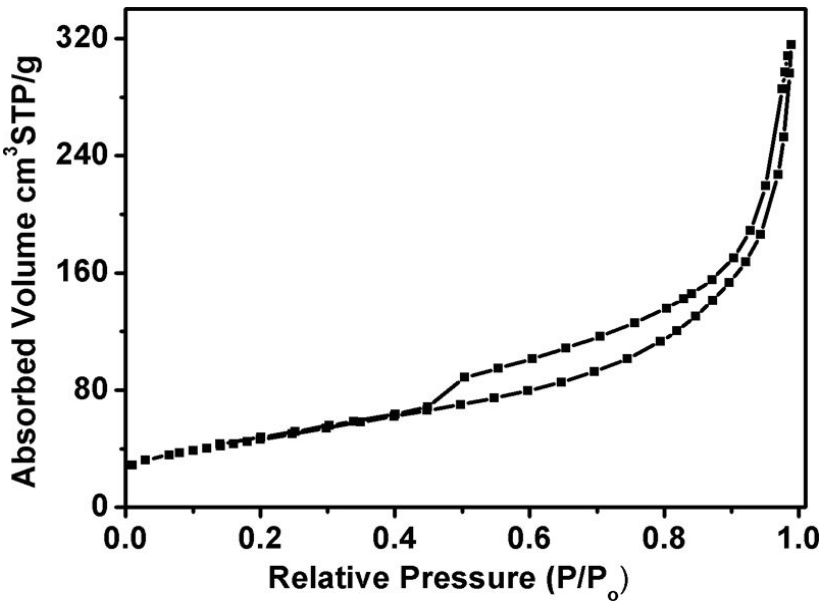

Fig. S5 N_2 adsorption isotherm of the synthetic CrN/GC-2-900 hybrid.

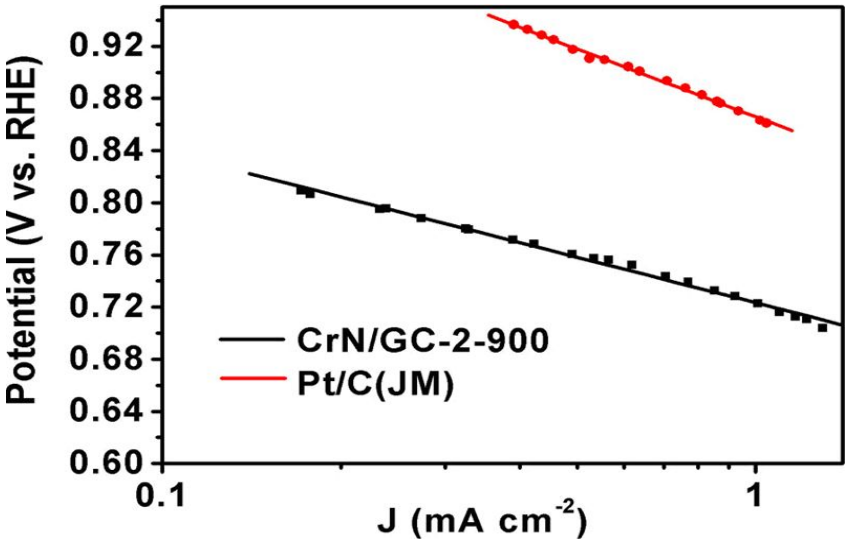

Fig. S6 Tafel plots for CrN/GC-2-900 and Pt/C catalysts.

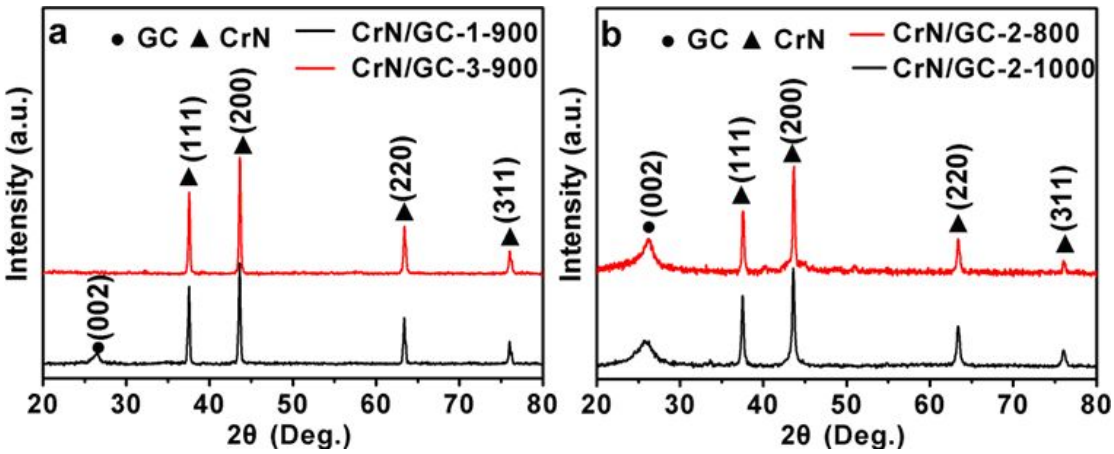

Fig. S7 XRD patterns of the CrN/GC samples synthesized from different experimental conditions: (a) CrN/GC-1-900 and CrN/GC-3-900 derived from 0.3 and 0.06 M $Cr_2O_7^{2-}$, respectively; (b) CrN/GC-2-800 and CrN/GC-2-1000 with a nitrided temperature of 800 and 1000 ^oC, respectively.

To investigate the effect of CrN content and treatment temperature on the ORR performances, the hybrids derived from different $Cr_2O_7^{2}$ concentrations and different nitrided temperatures were also prepared. The CrN/GC-1-900 and CrN/GC-3-900 hybrids are derived from 0.3 and 0.06 M $Cr_2O_7^{2-}$, respectively, CrN/GC-2-800 and CrN/GC-2-1000 hybrids are derived from a nitrided temperature of 800 and 1000 ^oC. (the detailed experimental conditions were listed in **Table S1**, and corresponding CrN content tests were displayed in **Fig. S1** and **Table S2**. All the hybrids exhibit the same peaks as shown in **Fig. S7**. The diffraction peaks at 37.5°, 43.6°, 63.4°, 76.0°can be assigned to the (100), (002), (101) and (311) facets of CrN with a face-centered cubic structure, which matched well with those reported in the JCPDS 03-065-2899. The peak at 2θ=26.4° is the (002) diffractions of graphitic carbon, demonstrating all the synthetic hybrids are composed of CrN and graphitic carbon with well crystalline.

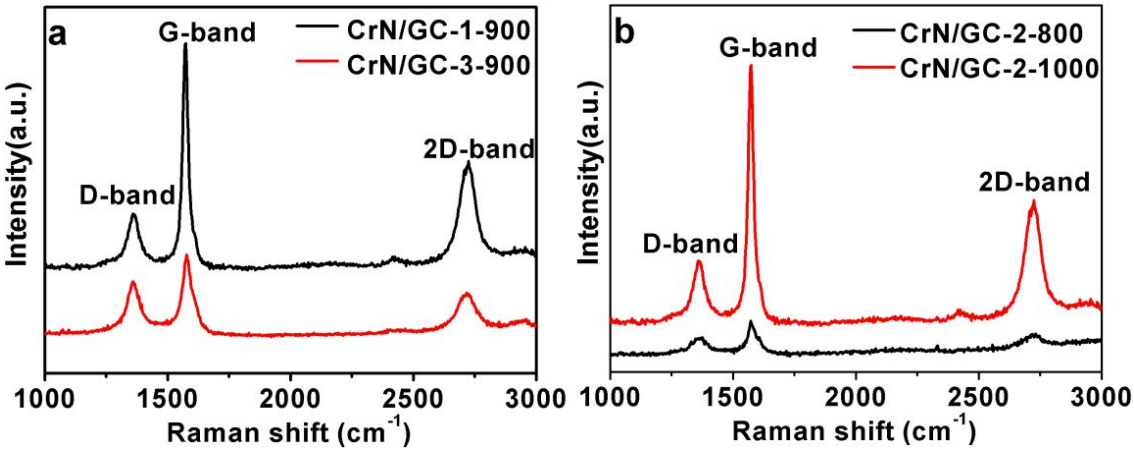

Fig. S8 Raman spectra of the CrN/GC hybrids synthesized from different experimental conditions: (a) CrN/GC-1-900 and CrN/GC-3-900 derived from 0.3 and 0.06 M $Cr_2O_7^{2-}$, respectively; (b) CrN/GC-2-800 and CrN/GC-2-1000 with a nitrided temperature of 800 and 1000 ^oC, respectively.

Raman analysis was carried out to understand the crystal structure of the obtained carbon materials. As can be seen from Fig. **S8**, all the hybrids show the similar peak of D-band, G-band and 2D-band. The results imply the well crystalline of the synthetic hybrids, which is consistent with the above XRD results in Fig. S7.

Table S4. The domain size of carbon nitrides on the basis of the ratio between the peak areas under the D-band and G-band in Fig 1b, Fig. S3b and Fig. S8.

Samples	Domain Size (nm)
CrN/GC-1-900	0.50
CrN/GC-2-900	0.77
CrN/GC-3-900	0.90
CrN/GC-2-800	0.83
CrN/GC-2-1000	0.51
GC	0.80

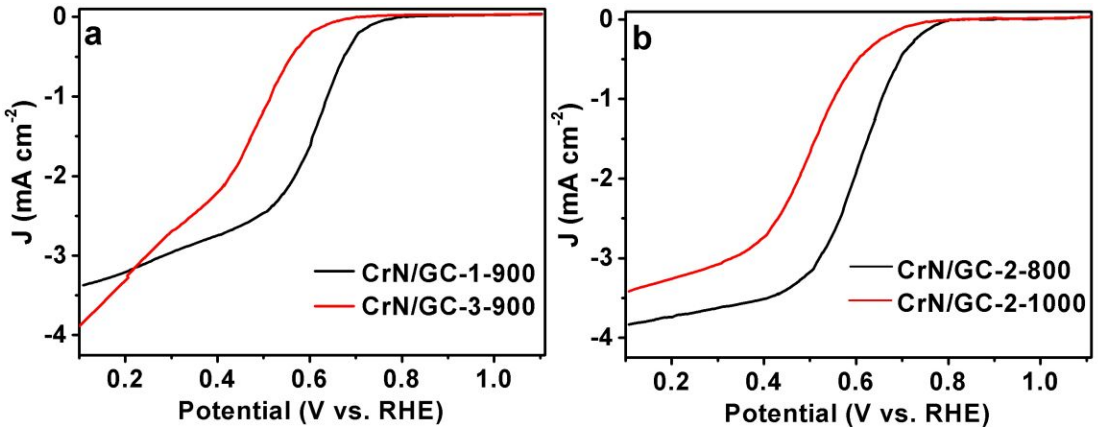

Fig. S9. LSV curves of the CrN/GC samples synthesized from different experimental conditions: (a) CrN/GC-1-900 and CrN/GC-3-900; (b) CrN/GC-2-800 and CrN/GC-2-1000 at a scan rate of 5 mV s^{-1} with a rotation rate 1600 rpm in O_2-saturated 0.1 M KOH electrolyte.

Table S5. The ORR performances of all the compared samples.

Samples	E_{onset} (V)	$E_{1/2}$ (V)	Electrons transfer number (n)	i_L (mA cm^{-2})
CrN/GC-1-900	0.80	0.63	3.87	3.36
CrN/GC-2-900	**0.86**	**0.70**	**4.10**	**3.93**
CrN/GC-3-900	0.73	0.50	3.52	3.81
CrN/GC-2-800	0.79	0.62	4.13	3.82
CrN/GC-2-1000	0.77	0.52	3.15	3.39
GC	0.58	0.45	2.89	-
Pt/C	0.98	0.80	3.98	3.68

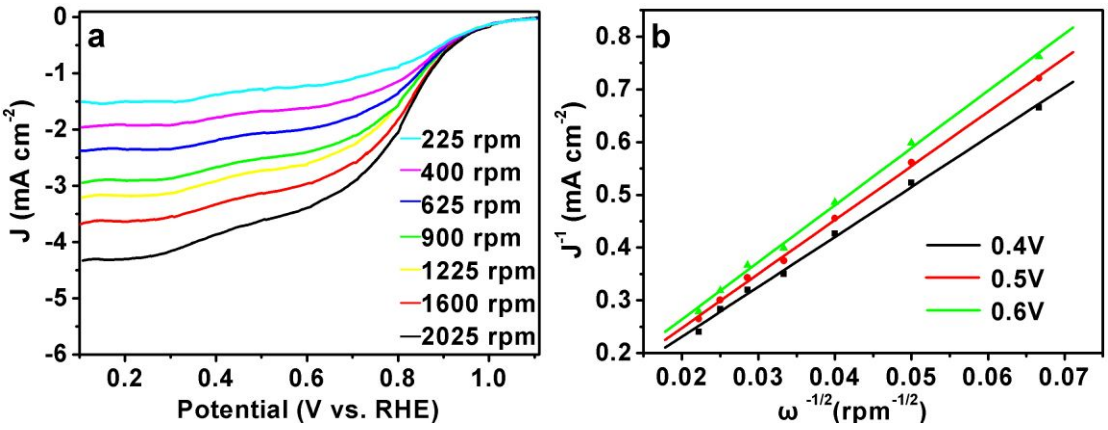

Fig. S10 (a) LSV curves recorded for Pt/C (40 wt %, JM) electrode in an O_2-saturated 0.1 M KOH solution at a scan rate of 5 mV s^{-1} and different rotation rates; (b) Koutecky–Levich plot of J^{-1} vs. $\omega^{-1/2}$ at different potential obtained from (a).

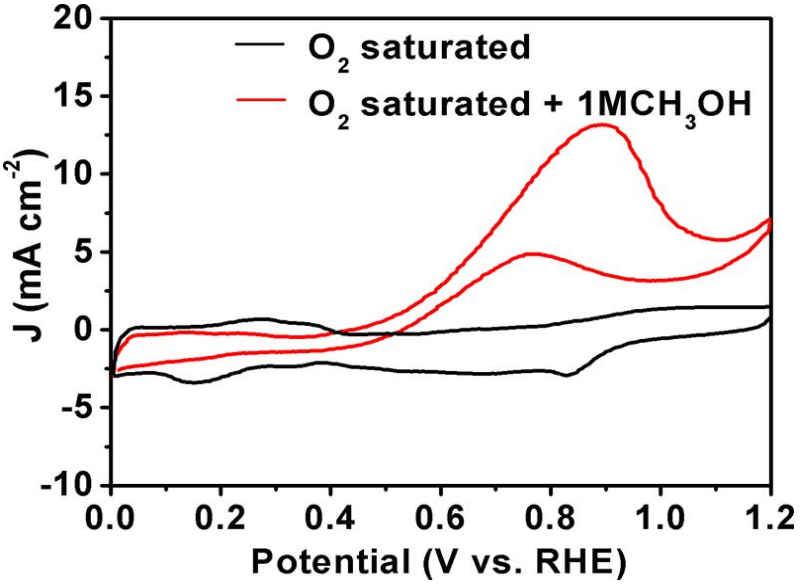

Fig. S11 CV curves of commercial Pt/C catalyst at a scan rate of 50 mV s^{-1} in O_2-saturated 0.1 M KOH electrolyte as well as O_2-saturated 0.1 M KOH with 1 M CH_3OH.

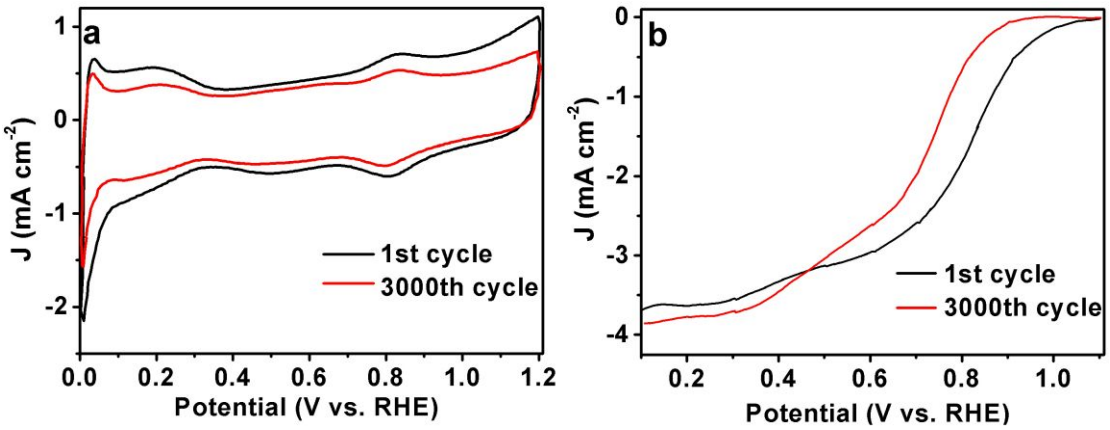

Fig. S12 Cyclic stability test of commercial Pt/C catalyst: (a) CV curves before and after 3000 cycles at a scan rate of 50 mV s^{-1} in N_2-saturated 0.1 M KOH electrolyte; (b) LSV curves before and after 3000 cycles in O_2-saturated 0.1 M KOH electrolyte at a rotation rate of 1600 rpm with a scan rate of 5 mV s^{-1}.

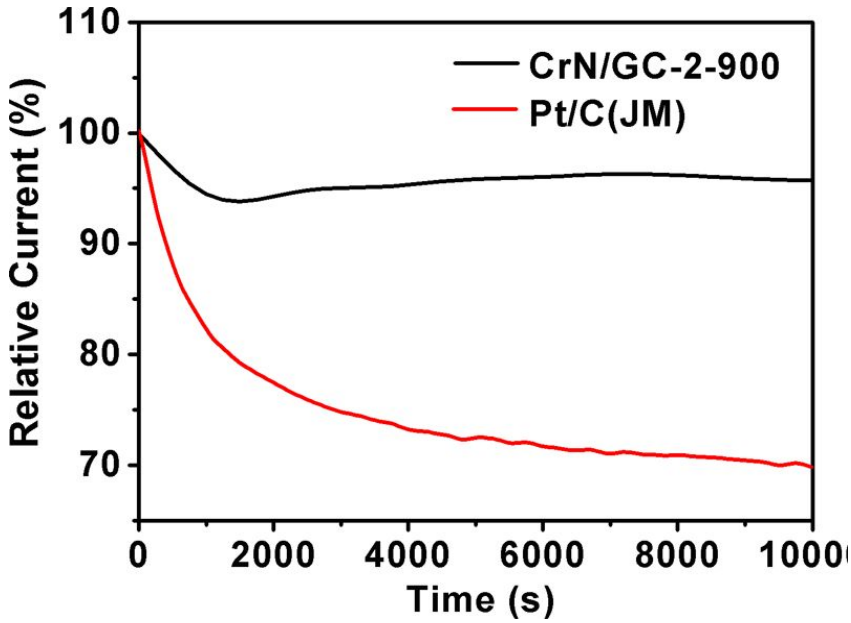

Fig. S13 Chronoamperometric responses for the CrN/GC-2-900 and commercial Pt/C electrodes in O_2-saturated 0.1M KOH electrolyte at 0.6 V (vs. RHE).

Chronoamperometric tests over 10000 s at potential 0.6 V (vs. RHE) for the catalysts were also used to estimate the durability of the catalysts, and the results are displayed in **Fig. S13**. It can be seen that the residual currents for the CrN/GC-2-900 catalyst is 95.7 % of its initial current density after 10000 s, which is much higher than that of Pt/C(JM) catalysts (70.1 % of its initial current density after 10000 s). The result demonstrated the excellent stability of the CrN/GC-2-900 catalyst compared with Pt/C(JM).

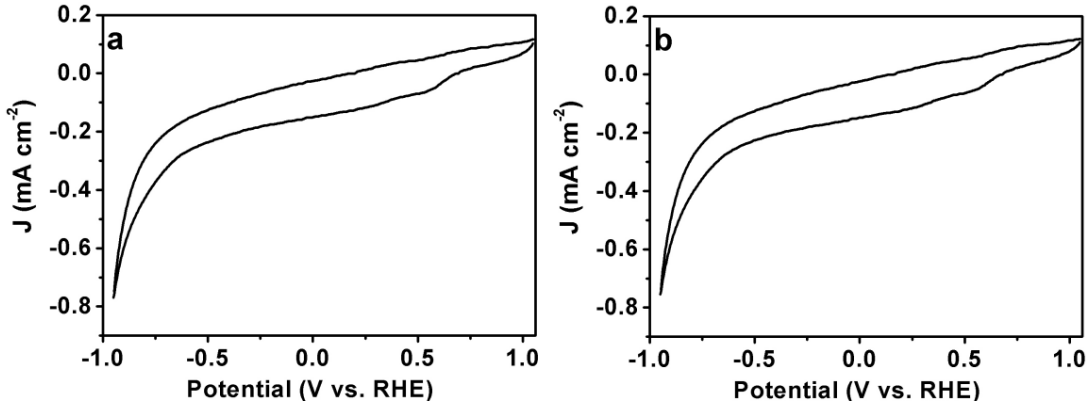

Fig. S14 The CV cures by using the bare glassy carbon electrode in the electrolytes after stability: (a) the 0.1 M KOH electrolyte of CrN/GC-2-900 tested after 3000 cycles, namely the electrolyte after Fig. 3f test; (b) 0.1 M KOH electrolyte after 10000 s Chronoamperometric responses for the CrN/GC-2-900 at 0.6 V (vs. RHE), namely the electrolyte after Fig. S13 test.

Notably, the Cr element in CrN is very stability under the present electrochemical test. To clarify this, we test the electrolyte after stability tests (Fig. 3f and Fig. S13) by using a bare glassy carbon electrode. As shown in **Fig. S14**, there is no obvious oxidation/reduction about Cr^{2+}/Cr^{3+} around -0.41 V. We also used ICP-AES to detect the electrolyte after Fig. 3f and Fig. S13 tests, the results show no Cr species could be tested. The above analyses further demonstrate the Cr in the CrN in indeed stability. Therefore, our present study indicates the CrN/GC hybrid could be used as a promising candidate for replacing Pt.

References:

[S1]. Y. Jiao, Y. Zheng, M. Jaroniec and S. Z. Qiao, *J. Am. Chem. Soc.*, 2014, **136**, 4394.

[S2]. W. Ding, L. Li, K. Xiong, Y. Wang, W. Li, Y. Nie, S. Chen, X. Qi and Z. Wei, *J. Am. Chem. Soc.*, 2015, **137**, 5414.

[S3]. J. Yin, L. Wang, C. Tian, T. Tan, G. Mu, L. Zhao and H. Fu, *Chem. Eur. J.*, 2013, **19**, 13979.